Revised version submitted to *The Astrophysical Journal*

SUCCESSIVE REFINEMENTS IN LONG-TERM INTEGRATIONS OF PLANETARY ORBITS

F. Varadi

Institute of Geophysics and Planetary Physics,
University of California, Los Angeles, Los Angeles, CA 90095-1567

B. Runnegar

Department of Earth and Space Sciences,
Institute of Geophysics and Planetary Physics Center for Astrobiology,
and Molecular Biology Institute,
University of California, Los Angeles, Los Angeles, CA 90095-1567

M. Ghil

Department of Atmospheric Sciences and
Institute of Geophysics and Planetary Physics,
University of California, Los Angeles, Los Angeles, CA 90095-1567
and
Département Terre-Atmosphère-Océan and Laboratoire de Météorologie Dynamique,
Ecole Normale Supérieure, 75213 Paris Cedex 05, France

ABSTRACT

We report on accurate, long-term numerical simulations of the orbits of the major planets in our solar system. The equations of motion are directly integrated by a Störmer multi-step scheme, which is optimized to reduce round-off errors. The physical models are successively refined to include corrections due to general relativity and the finite size of the lunar orbit. In one case, the Earth–Moon system is resolved as two separate bodies and the results are compared to those based on analytically averaging the lunar orbit. Through this comparison, a better analytical model is obtained. The computed orbits are in good agreement with those of previous studies for the past five million years but not for earlier times. The inner planets exhibit chaotic behavior with a Lyapunov time of exponential separation of nearby orbits equal to about 4 million years.

Modeling uncertainties and chaos in the inner solar system restrict the accuracy of the computations beyond the past 50 million years. We do not observe marked chaos in the motion of the Jovian planets in our 90-million year integration, and infer that the Lyapunov time for those planets is at least 30 million years.

Subject headings: methods: N-body simulations — solar system: general

1. INTRODUCTION

1.1. Background and Motivation

The long-term evolution of the orbits of the major planets is an important problem for astronomy, as well as the geosciences. Numerical simulations of planetary orbits have become fairly common in the past decades, but their main goal so far has been the understanding of orbital dynamics and not necessarily very high accuracy. It does not particularly matter for an astronomer whether Earth's orbital eccentricity was low or high at a given time, as long as the reasons for its variations are well understood. For the geosciences, however, the actual numbers are more important since geological records of isotope ratios are routinely compared to and interpreted using orbital variations (Hays, Imbrie & Shackleton 1976; Berger et al. 1984; Imbrie et al. 1992, 1993). The exact connections between Earth's orbital variations, its climate evolution, and its geological record are still a matter of debate (Ghil 1994; Gildor & Tziperman 2000; Zachos et al. 2001). Paleoclimatologists need therefore more accurate orbital data, covering longer time intervals, as they try to unravel the complex, evolving interactions between Earth's orbital parameters and climate.

For achieving high accuracy, we had to carefully consider both the physical model used in computing accelerations and the simulation methodology. Our choice for the latter is an improved version of the classical Störmer scheme (e.g., Quinlan 1994), which two of the present authors had used in previous studies (Grazier et al. 1995; Varadi, Ghil & Kaula 1999a). The real difficulty is with the physical model. There are a number of small corrections to the equations of motion which could have noticeable effects on the long-term evolution of orbits (e.g., Quinn, Tremaine & Duncan 1991; Laskar 1999).

Our approach here is to gradually refine the physical model, until corrections become unimportant compared to integration errors and the effects of chaos. We have not reached that point yet. At present, it is the uncertainties in modeling the Earth–Moon system that limit the validity of our simulations and not integration errors. This is so even without considering tides, as we treat the planets as point masses for now. Chaos (e.g., Lichtenberg

& Lieberman 1992), however, further constrains the validity of our numerical results, making them less reliable beyond about 70 million years (Myr). Overall, we believe that the details of our computations can be trusted for the past 50 Myr, except for Mercury's position along its orbit.

Accuracy can also be important for astronomers, however. For certain problems of solar system dynamics, more accurate orbital computations can make not only quantitative but also qualitative differences. When the numerical evidence that is available to draw a conclusion is only marginal, one has to worry about small effects. For instance, in our most elaborate physical model the motion of the Jovian planets does not appear to be chaotic. This contradicts, on the face of it, the results of Sussman and Wisdom (1992) and Murray and Holman (1999) who used simpler models, different simulation methods, different initial data, and a different way of detecting chaos. We also have to emphasize that our 90-Myr simulations are not long enough to rule out chaotic behavior with Lyapunov time (i.e., inverse of leading Lyapunov exponent) longer than about 30 million years. Furthermore, the solar system as a whole is chaotic since the inner solar system is chaotic. The effect of the latter on the motions of the Jovian planets might be difficult to detect, for two reasons: (i) the relatively small mass of the inner planets; and (ii) the fact that their effect has to compete with integration errors.

Before going any further, it is worth demonstrating the differences between our results and earlier ones. In Fig. 1, Earth's orbital eccentricity is compared for a short time interval (0.3 Myr) around 24 Myr in the past, which is the traditionally accepted age for the Oligocene–Miocene boundary in geology (23.8 Myr, according to Berggren et al. 1995; but see also Shackleton et al. 2000 for a different view). Laskar's (1990, 1999) solution appears to be quite different from ours, even when we use the analytical Earth–Moon model of Quinn et al. (1991), which is supposedly very similar to the one used by Laskar (see also Laskar, Quinn & Tremaine 1992). Moreover, our results, when using the model of Quinn et al. (1991), still disagree to a noticeable extent with the present paper's simulation in which the Earth and the Moon are resolved as separate bodies. Our improved analytical model, obtained through such comparisons, seems to work much better, in a sense that will be explained in Secs. 5.3 and 6.

In the next subsection, we briefly discuss orbital and climate variations. In Sec. 2, we consider the problem of achieving high accuracy, both in terms of methodology and physical models. The numerical scheme and the code are described in Sec. 3, while the accuracy of our simulations and the effects of chaos are analyzed in Sec. 4. The details of the physical models are discussed in Sec. 5. Comparisons between simulation results are made in Sec. 6 and conclusions follow in Sec. 7. Most of the technical details regarding long-term, direct

integrations of orbits by multi-step schemes have been presented in other papers (e.g., Quinn et al. 1991) and we do not repeat them here. Several data sets from our simulations are freely accessible[1]. and others can be made available upon request.

1.2. Orbital and Climate Variations

Since the present study is partly motivated by problems in paleoclimatology, a brief sketch of this field is worth a digression. The largest climate changes in the past few Myr were in the form of transitions between warmer, relatively ice-free episodes like the present and the much cooler, glacial episodes when large portions of North America, northern Europe and Asia were covered with ice sheets. The astronomical theory attempts to explain the occurrence and cyclicity of ice ages by purely external causes, namely, variations in the Earth's orbit and rotation axis (Milankovitch 1941; Imbrie & Imbrie 1986; Zachos et al. 2001). Such changes modulate the amount of solar radiation reaching the Earth's surface, both its globally averaged value and its spatio-temporal distribution. For instance, an increase in obliquity results in larger differences between the seasons, especially for high latitudes.

There are three astronomical variables used in paleoclimatology: the obliquity, the eccentricity multiplied by the sine of the longitude of perihelion, measured from the vernal equinox, and eccentricity itself. The annually averaged insolation integrated over the whole surface of the Earth is a function of eccentricity and semi-major axis. Since fractional variations of the latter are very small for Earth, the main astronomical variable of interest in paleoclimatology is eccentricity.

The theory explains many features observed in the geological record of the past 2.5 Myr. Obliquity cycles, of about 40,000 years, for instance, can be detected in various ice and deep-sea drill core data. But the largest variations, with periods around 100,000 years, remain difficult to explain by orbital variations alone, as are large variations with periods as short as a few thousand years (Ghil & Childress 1987; Ghil 1994). Nevertheless, it is routine in the geosciences to interpret geological records in terms of orbital variations and even to tune (Imbrie et al. 1992, 1993; Shackleton et al. 1999) or calibrate (Renne et al. 1994) the age of the records according to these variations. This is partly through necessity since only stratigraphic thickness can be reliably measured in geology and its relationship to age has to be inferred indirectly.

There are other theories of glaciation cycles, which take into account the internal dy-

[1]http://www.astrobiology.ucla.edu/SSO

namical processes of the climate system, while not discounting orbital forcing. Changes in ice cover lead to variations in planetary albedo, which, in turn, affects temperature (Budyko 1969; Sellers 1969). The latter influences the hydrological cycle and, hence, the growth of ice sheets (Ghil & Le Treut 1981; Gildor & Tziperman 2000). Another important component is the isostatic rebound of the lithosphere after the melting of ice sheets (Weertman 1976; Birchfield & Ghil 1993). Some models with such feedbacks can reproduce the 100,000-year cyclicity as a result of nonlinear interactions between very small insolation changes due to variations in Earth's orbital parameters and the internal oscillations of the climate system (Ghil 1994; Gildor & Tziperman 2000).

The ultimate explanation for the 100,000-year cyclicity in glaciations that dominated the past few Myr is yet to be found. Nevertheless, the astronomical calibration of the geological record is already in progress for the much older Oligocene and Miocene times, part of which is shown in Fig. 1. Interestingly, the prolonged eccentricity minimum around 23.9 Myr in our results appears to be very close to the traditional age of the Oligocene–Miocene boundary (23.8 Myr), as well as to the Mi-1 cooling event which is represented by extreme values in δ^{18}O and δ^{13}C records (Zachos et al. 2001). Shackleton et al. (2000) used Laskar's (1990, 1999) orbital simulations to calibrate the Oligocene–Miocene time scale and concluded that the boundary between the two is about 1 Myr younger than the traditionally accepted age. This discrepancy will be dealt with in detail elsewhere.

2. GENERAL CONSIDERATIONS

2.1. Analytical vs. Numerical Methods

There are two main approaches to compute planetary orbits accurately for long times. Laskar (1990) first orbitally averaged the mutual perturbations between planets, based on the work of Duriez (1982), and then numerically integrated the resulting secular system. The latter is represented as truncated series expansions in planetary masses, orbital eccentricities and inclinations. Laskar's results have replaced to a large extent the classical ones of Berger (1978) and Bretagnon (1982) as the main reference in the geosciences for the past evolution of planetary orbits (see above).

The other approach is the direct integration of the equations of motion. We consider the work of Quinn et al. (1991) to be the most advanced in this direction and we follow it in many respects. Since their work, however, there has been considerable increase in the speed of computers, allowing more extensive studies and much longer simulations.

For the most part, the technical details of our simulations are straightforward. As

opposed to Laskar's (1990) averaging, we directly integrate the equations of motions, as did Quinn et al. (1991). We have carried out orbital averaging in the past for various problems, sometimes using series expansions with hundreds of thousands of terms (Varadi, Ghil & Kaula 1995; Ghil, Varadi & Kaula 1996). We found that straightforward averaging over the orbital time scale fails for the case of our solar system because Jupiter and Saturn are too close to the 5:2 mean-motion resonance (Varadi et al. 1995, 1999a). It is this same 5:2 near-resonance between Jupiter and Saturn that led Laskar (1990) to adjust his secular system to better match his results to those of direct numerical integrations. Hence, we follow Quinn et al. (1991), but employ a new, improved integrator and faster computers. In one simulation, we even resolved the Earth–Moon system as two separate bodies, resulting in a ten-fold decrease in speed. Such a simulation would have been quite impractical until now.

2.2. Numerical Issues

The goals regarding accuracy have to be realistic. Despite progress in the past decade, we face essentially the same problems as Quinn et al. (1991). We use double-precision floating point arithmetical operations on ordinary digital computers since quadruple-precision floating point arithmetic is not available in off-the-shelf hardware. At every step there is a loss of information in the form of round-off error, as only a finite number of digits can be retained for subsequent integration steps. These errors accumulate over time and their effects can only be minimized, but not completely overcome. The presence of chaos, moreover, severely limits the accuracy of orbital integrations on the time scale of millions of years. Chaos causes initial errors to grow exponentially in time, and so the simulated orbits diverge from the correct ones.

Since we had to integrate for millions of years and carry out several simulations, we had to select a relatively fast integration scheme. This, together with the goal of high accuracy, naturally led us to a multi-step scheme. We use a Störmer scheme (Quinlan 1994) because its properties are well-known and we are familiar with it. Another possibility would have been to use a symmetric method (Quinlan & Tremaine 1990), which has several advantages, but also a major drawback: the principal roots of the method on the unit complex circle can lead to resonant interactions, as shown by Quinlan (1999). When the number of steps per orbit is resonant, the integration error is orders of magnitude larger than that for a comparable Störmer scheme. It is difficult to avoid these resonances.

We have also used various versions of the Wisdom & Holman (1991) mapping in other projects (e.g., Musotto et al. 2002), but not in the present one. The mapping is a symplectic scheme specific to perturbed planetary motions which, as the name implies, preserves the

symplectic structure (Arnold 1978, 1988) associated with the Hamiltonian equations of motion. The mapping has two main advantages over other, more general schemes, as pointed out by Kinoshita et al. (1991). One is that the unperturbed Keplerian motions are computed analytically and not numerically. The other one is that the error is proportional to the magnitude of the perturbations due to interactions. This advantage is diminished, however, for higher-order versions of the mapping, as was shown by Kinoshita et al. (1991) as well. Higher orders imply higher powers of the step size in the leading error terms, which are also multiplied by the magnitude of the perturbations. Hence, error becomes strongly dependent on step size and less dependent on the magnitude of perturbations. Essentially the same argument applies to higher-order mapping schemes (e.g., Laskar & Robutel 2001).

The Wisdom-Holman mapping now has a number of variants. For instance, Varadi, Ghil & Kaula (1999b) showed that using mass-weighted symplectic forms naturally removes singularities associated with vanishingly small masses. Malhotra (1994) discussed nonsymplectic versions. Saha and Tremaine (1994) introduced a Hamiltonian for general relativity effects, although the equations of motion that correspond to their Hamiltonian are not the same as the ones used by Quinn et al. (1991) and us. A particular feature of mapping techniques is that a large part of the error is in the form of spurious, high-frequency oscillations associated with the discrete nature of mappings. Adjusting both initial data and integration output is a way to reduce the amplitude of such oscillations. The initial-data problem can be dealt with by "warming up" the integrations (Saha and Tremaine 1992). Symplectic correctors (Wisdom, Holman & Touma 1996) can correct both initial data and the integration output. These correctors, however, do not reduce long-term errors since they eliminate only high-frequency variations from the integration output; nor are they simple to implement.

Perhaps the least understood aspect of the Wisdom-Holman mapping is step-size resonances, which are similar to those in symmetric multi-step schemes. While their effects should decrease very rapidly with decreasing step size (Wisdom & Holman 1992), we are not convinced that the issue is fully resolved. It appears, therefore, that adopting an improved version (Grazier et al. 1995; Goldstein 1996) of the trusted Störmer integration scheme serves the goals of this project the best.

2.3. Physical Model Design

We can only simulate the solar system as we know it today, without drastic changes in its basic properties. We cannot completely rule out that additional planets existed and were ejected in the past. Likewise, relatively close encounters with a number of stars could have taken place in the past 200 Myr (Garcia-Sanchez et al. 2001). It is certain that small bodies

collided with the major planets and caused small changes in their orbits, but we cannot model those impacts individually. The cumulative effect of small impacts can be modeled through orbital averages, allowing to study their influence on orbital evolution and resonances (Wolansky et al., 1998). To obtain robust answers, however, we would have to compute a large ensemble of simulations with random initial data and parameters of the system, as well as stochastic forcing for impacts and the effects of passing stars. Such large ensembles of predictions are routinely used today in extended-range weather prediction (Kalnay 2002), but are beyond our computational resources in celestial mechanics.

It is difficult, even in principle, to estimate the importance of small corrections in the equations of motion on the long-term evolution of planetary orbits. Comparing the magnitude of such terms to those representing Sun–planet gravitational forces is meaningless: consideration of the latter terms only leads to a degenerate problem since the orbit of the planet does not change in time. Any additional force, e.g., perturbations by other planets, breaks this degeneracy and allows the orbit to evolve. Furthermore, the goal here is to compute secular changes and hence variations on the orbital time scale are not so important. For this reason, Laskar (1999) compares the estimated secular effects of small corrections to the secular effects of planet–planet interactions. Short-periodic variations, however, interact with each other and can contribute sizable secular changes. It seems that the most reliable way to assess the effect of a small correction is to include it in the equations of motion directly and carry out simulations.

Our approach in this project is to gradually refine the physical model until the resulting changes in the orbits are smaller than the uncertainties caused by chaos and numerical errors. Even if one finds our simulation errors to be larger than desired, they are still much smaller than the effects of the small corrections in the equations of motion that we discuss in this paper.

Some of the refinements we introduce can only be approximations, since we do not have accurate models for all the forces acting on solar system bodies. Nevertheless, one can employ even relatively poor approximations for small model corrections in order to assess the effect of these corrections. Next, one can try to improve the physical modeling of what is found to be important and may ignore the rest. Laskar (1999) provides an excellent overview of many small corrections that one might have to take into account, but even his list does not include, for instance, the interaction of the solar wind with planetary magnetospheres. J. Raeder's (2001, private communication) order-of-magnitude estimate of this effect gives an acceleration that is comparable to photon radiation pressure.

Besides Newtonian gravitation between point masses, the majority of our simulations include corrections due to general relativity for Sun–planet accelerations and the finite size of

the lunar orbit. In order to assess the effects of such small corrections, they were incorporated into increasingly more elaborate models, starting with the case of Newtonian gravitation only. We compare Earth's smoothed orbital eccentricity across simulations since this is the main variable of interest. Except for the improved model of the Earth–Moon system, our equations of motion are the same as in Quinn et al. (1990).

The simulations we performed are summarized in Table 1. Their differing lengths are due to several factors. When the Earth and Moon are resolved (R5), the simulation makes very slow progress and hence it is short compared to others. The first integration, R1, was a test case and is used only as a base line for comparisons. The others were allowed to run until a decision could be made regarding the next simulation. The numerical accuracy of the simulations was assessed by comparing the results of R2 and R3. These two simulations share the same physical model, which appears to be sufficiently accurate for such a purpose, and differ only in the step size (see Figs. 2 and 3 and their discussion in Sec. 4).

3. THE NUMERICAL SCHEME AND THE CODE

We employed a modified Störmer scheme, which is an explicit method for systems of second-order differential equations. The Störmer scheme is analogous to the well-known explicit Adams methods (Gear 1971) that are widely used for systems of first-order equations. The coefficients of the classical Störmer scheme, however, exhibit large oscillations (Quinlan 1994). We employed an improved version that is optimized for reducing round-off errors (Grazier et al. 1995; Goldstein 1996). The new scheme has been used in previous studies (Grazier et al. 1995, 1999a,b; Varadi et al. 1999a) and the source code of a particular implementation in C is provided by the first author of the present paper (Varadi 1997[2]). The actual code used in the present work is a modified version of the one above. The integrations are carried out on ordinary Sun workstations and a Pentium-processor-based PC.

There are a number of issues that affect accurate, long-term simulations. The initial array of positions, which has to be determined with high accuracy, was computed by using quadruple precision numbers and a Stoer-Bulirsch-Gregg extrapolation scheme (Hairer, Norsett & Wanner 1993). As the integration progresses, the array of positions and velocities was updated at each integration step and saved, along with other data, at certain time intervals and in binary format. This allowed the simulation to be continued without any loss of information after inevitable interruptions. The entire simulation output was saved in binary

[2]http://www.astrobiology.ucla.edu/∼varadi/NBI/NBI.html

format; particular results of interest were extracted using a separate code. When necessary, the latter also performs simple transformations, such as rotation from the J2000 coordinate frame used in the integration to another one aligned with the invariable plane of the solar system.

Any numerical scheme has both truncation and round-off errors. The numerical solution can be expressed as a truncated power series in the step size and the number of terms which match the actual solution corresponds to the order of the method. The remainder of the series is the local truncation or systematic error. Round-off is due to having only finitely many digits to represent a real number on a digital computer. This leads to the loss of least significant digits in each arithmetic operation. Smaller step sizes imply smaller truncation but a larger accumulation of round-off errors and, hence, there is always an optimal step size (Isaacson & Keller 1994).

The optimal step size for our modified Störmer scheme corresponds to about 1000 steps per Keplerian orbit (Grazier et al. 1995; Goldstein 1996). With this choice, the integration error for a single step is smaller than the smallest number in double-precision representation. When the range of orbital periods in the system is large, the step size should be optimized for the smallest orbital period. This choice leads to larger round-off error for planets with larger orbital periods. The present work used the new Störmer scheme at order 14, with step sizes of 0.3125 or 0.25 days in most cases. These values are nearly optimal for Venus and Earth and slightly suboptimal for the other planets. With these step sizes, it takes about one wall-clock day to integrate the motion of the major planets for one Myr. When the motions of Earth and Moon are resolved, the step size was taken to be 0.03125 days, with a corresponding ten-fold decrease in speed and an increase in accumulated round-off error.

Although positions and velocities are available at each simulation step, saving all of them is impossible because of file size limitations. It is customary (Quinn et al. 1991) to compute orbital elements every twenty or so days and save them only every few hundred years. One has to ensure that the final, undersampled output is free of signal aliasing (Proakis and Manolakis 1996). Furthermore, the goal is to compute the low-frequency variations in orbital elements and, hence, the high-frequency contributions can be discarded. The low-frequency variations were computed by standard low-pass filtering. We refer to the low-pass filtered orbital elements as smoothed and call the instantaneous, unfiltered orbital elements unsmoothed.

The smoothed orbital elements were computed as follows. First, the output was decimated to have the positions and velocities of all the bodies every 25 days. From these, we determined the semi-major axes and the components of the angular momentum and Laplace vectors. Except in the case when the Earth–Moon system was resolved into two separate

bodies, there were no large variations with periods shorter than 25 days in these orbital elements. Hence the primary decimation, with output every 25 days, is not expected to introduce any aliasing.

Next, a standard low-pass filter (Proakis and Manolakis 1996) with 60,000 coefficients was applied to the 25-day simulation output, which eliminates all variations with periods shorter than 342 years. The low-pass filtered signal was then decimated in turn to produce the final output of orbital elements every 342 years. It is worth noting that a single output value when using the 25-day sampling rate contributes only to 13 output values at the 342-years sampling rate. Hence, the overhead associated with low-pass filtering is barely noticeable. Smoothed orbital elements are not available for the first 4,400 years, because of the filter's broad window.

When resolving the Earth–Moon system, we computed the orbital elements of the Earth–Moon barycenter, rather than those of Earth's orbit. The motion of the Moon introduces changes in the orbital elements which are not removed by low-pass filtering. These additional variations, however, have very small amplitudes and do not change the results noticeably.

4. NUMERICAL ACCURACY AND CHAOS

Many routine tests were carried out to validate the code, e.g., by comparing its output to those of other methods. A more fundamental way to test the code and estimate actual integration errors is to compute the same orbits with the same physical model but with two different step sizes. This provides a much more reliable estimate of integration errors than monitoring first integrals, such as total energy. The latter is not even conserved in our physical models due to the effects of general relativity. It is not clear, though, which variables best describe long-term accuracy.

We are interested primarily in the shape and orientation of orbits in an average, secular sense and much less in short-periodic changes. The position of a planet along its orbit reflects both short- and long-term changes. It also has the largest errors since longitude along the orbit is a linear function of time, being essentially the time integral of the semi–major axis. Even when the errors in the latter are uniformly small over the full length of the integration, the error in the longitude will grow. In contrast, shape–orientation orbital elements, especially their smoothed version, are expected to have much smaller errors.

Quinn et al. (1991) estimated errors by computing fractional position differences which are dominated by differences in longitudes. In their simulations, such differences were of the order of 10^{-5} or less after one Myr. In the case of Mercury, however, they were of order 0.1;

these authors also estimated that after 3 Myr the probable error in Mercury's longitude is about 1 radian. It appears, as they note, that this error was due to an instability in their integration scheme. Step-size resonances (Quinlan 1999) might explain this instability.

We computed fractional position differences between two simulations, R2 and R3 (see Table 1) with step sizes of 0.3125 and 0.25 days, respectively. In Fig. 2a, one can observe that after 1 Myr the errors are around 10^{-5} for all planets shown, including Mercury. Therefore, our integration is more accurate for Mercury than that of Quinn et al. (1991): it performs in every respect as expected of a high-order multi-step scheme. Mercury is the worst case in our simulations, having estimated longitude errors around 0.1 after 10 Myr.

For longer time intervals, up to about 55 Myr ago (Fig. 2b), the errors remain below 10^{-3}, except in the case of Mercury, where they grow to unity after 30 Myr. Our step size was chosen to be optimal for the Earth and it is larger than optimal for Mercury, leading to larger truncation errors. Yet these errors do not degrade the accuracy of the simulations for the other planets, since Mercury's mass is quite small. One can also observe a steep increase in the differences between the simulations, for Mercury, Venus and Earth, which starts around 55 Myr ago.

Compared to the longitudes, our results are much more accurate for the shape and orientation of orbits. In Fig. 3, the magnitude of the differences in vector eccentricities are plotted for the three planets, both smoothed and unsmoothed, using the same two integrations as in Fig. 2. Vector eccentricity is defined as the Laplace vector divided by the semi-major axis. Overall, vector eccentricity errors are much smaller than position errors, even when taking into account that vector eccentricity has a smaller average value. In the case of Mercury (panel a), the unsmoothed vector eccentricity exhibits larger initial differences because it includes short-periodic longitude errors. The differences grow polynomially in time for the first 50 Myr, at which point they are overtaken by smoothed vector eccentricity differences; the latter have smaller initial values but grow exponentially, i.e., linearly on the logarithmic scale of the plot.

The results for the Earth (Fig. 3b) are similar to those for Mercury, only the growth in the unsmoothed vector eccentricity errors at the beginning is slower. For both planets, the initially very small differences in the smoothed vector eccentricities grow exponentially. The nearly straight line up to 50 Myr is due to the chaotic nature of the orbital dynamics of the inner solar system.

Integration errors accumulate polynomially in time and are responsible for the initially logarithmic behavior of differences in Fig. 3. The presence of these errors, however, is analogous to integrating the system with slightly different initial data. Deterministic chaos

causes the exponential separation of the two solutions, which eventually overwhelms the additional integration errors that grow polynomially (see also Laskar 1999). Chaos also explains the sudden increase in the fractional position errors around 55 Myr (Fig. 2b). The Lyapunov time scale of the observed chaos, given by the inverse of the leading Lyapunov exponent, is about 4 Myr. This is in agreement with previous results (Laskar 1990; Sussman and Wisdom 1992) and goes to show that what really limits the accuracy of the simulations is not integration errors but chaos.

In Fig. 3c, we plot the differences in vector eccentricities for the case of Uranus. For about the first 30 Myr the differences are larger than in the case of Earth. Since the integration step size is smaller than the optimal value for Uranus, the round-off error is larger. There are also large, position-dependent perturbations between the Jovian planets, such as the 5:2 orbital near-resonance between Jupiter and Saturn and the 2:1 near-resonance between Uranus and Neptune, which are not removed by smoothing.

The overall behavior of the curve for Uranus appears to be logarithmic. This behavior indicates the absence of chaos up to 90 Myr and seemingly contradicts the results of Murray and Holman (1999), who detected chaotic behavior with a Lyapunov time around 7 Myr. There are important differences, however, between their study and the present paper. Our physical model includes the inner planets and also detailed corrections due to general relativity, while theirs did not. According to M. Holman (2001, private communication), their initial data were also different, which might play a role in a system whose phase space contains both chaotic and regular regions (Lichtenberg & Lieberman 1992). This is reinforced by the earlier results of Sussman and Wisdom (1992) who found that the Lyapunov time for the Jovian planets in their simulations depended on the integration method and the step size they used and varied from 3 Myr to infinity; the latter means absence of chaotic behavior. We also note that we do not observe the effect of inner solar system's chaotic behavior on the motions of the outer planets because it is too small compared to integration errors.

Most importantly, we may not be able to observe chaos in a 90-Myr integration if its Lyapunov time is long enough. Furthermore, the Lyapunov time can only be estimated from a relatively short model run even when the motion is undoubtedly chaotic. As a general rule, the initial portion of the simulation output is dominated by integration errors and, hence, the curves such as those in Fig. 3 initially exhibit logarithmic behavior. When the motion has sufficiently strong chaotic components, one expects to see linear increase after the initial logarithmic one. The picture is complicated by fluctuations, such as temporary decreases as the phase-space trajectory passes near hyperbolic structures (e.g., Varadi et al., 1999a). Sometimes (e.g., Sussman and Wisdom 1992) there are changes in the slope of linear increase. The curve of smoothed differences in vector eccentricities for Earth, shown

in Fig. 3b, gives 4.2 Myr as the Lyapunov time when computed for the time interval between 5 and 55 Myr. In the case of Mercury, the initial logarithmic component dominates until 25 Myr and the Lyapunov time is 3.5 Myr when computed for the time interval between 25 and 60 Myr. Given the uncertainties in computing Lyapunov times, our values are not significantly different from the 4 Myr reported by Sussman and Wisdom (1992) or even the 5 Myr of Laskar (1990).

The curve for Uranus Fig. 3 could be interpreted as either purely logarithmic behavior with fluctuations or initially logarithmic behavior overtaken by a very small linear increase. Assuming linearity for the time interval between 30 and 90 Myr yields 30 Myr as the Lyapunov time. This represents therefore a lower bound on Lyapunov time in the case of the Jovian planets.

In summary, our simulation errors behave as expected. Fractional position errors are around 10^{-3} or smaller for the first 50 Myr, except for Mercury. Eccentricities exhibit much smaller errors, which indicates that the main error is in the longitudes and not in the shape and orientation of orbits. The ultimate obstacle to achieving higher accuracy is chaos and not simulation errors, assuming that we have a sufficiently accurate physical model.

5. PHYSICAL MODELS

5.1. Initial Data

For accurate initial data, one has to rely on planetary orbital ephemerides (Seidelmann 1992), such as DE405 (Standish 1998[3]). The DE405 ephemerides are based on what is probably the most accurate physical model, but we cannot employ this model in our work, as it is too computationally expensive for long-term integrations. In DE405, corrections for general relativity are included for all planets and the Moon, leading to force terms in which three bodies are involved, as opposed to our model's two-body interactions.

We took the actual numbers for masses, positions and velocities directly from the binary ephemeris files. The integrations start at the same epoch as DE405. The Digital Ephemeris uses Astronomical Units and days as units for distance and time, respectively, which we also adopted. By definition, one ephemeris year is 365.25 ephemeris days (Seidelmann 1992); this is only a matter of practical convention and has no bearing on the length of the year in terms of Earth's rotation.

[3]ftp://navigator.jpl.nasa.gov/ephem/export/de405.iom

5.2. General Relativity Effects

We assume general relativity — as opposed to one of the competing theories — to be correct and use standard post-Newtonian approximations (Will 1981; Soffel 1989), as did Quinn et al. (1991). Only corrections for Sun–planet interactions are taken into account. In Fig. 4, we plot Earth's orbital eccentricity for a model with corrections arising from general relativity (R3) and one without (R1). The discrepancy grows quite rapidly and after 2 Myr the two curves bear only an overall, qualitative resemblance to each other.

The general relativity effects are much smaller for the outer planets but not negligible. In Fig. 5, we plot the difference in Jupiter's orbital eccentricity between the same two simulations. One can observe a pattern which is typical when the difference in the two time series is due to slightly different frequencies. The amplitude of the difference grows linearly in time; oscillations due to the beating between the two frequencies are superimposed on this linear trend. After about 80 Myr, the difference is almost 4% of Jupiter's present orbital eccentricity. It is obvious, once more, that our outer solar system, which does not appear to be chaotic, is different from the chaotic one of Murray and Holman (1999).

5.3. The Earth–Moon System's Effects

The Moon is the largest satellite relative to its planet in the solar system; it also has a relatively large orbital radius. In the simplest approximation, one can replace the Earth and the Moon with a fictitious body at their barycenter, as it was done in our simulations R1–3. Next, averaged models for the lunar orbit can be used, as we did starting with the R4 simulation. We followed therein the work of Quinn et al. (1991) and used the same model, which is based on a simplified version of Hill's lunar theory (Brouwer and Clemence 1961). In R4, we added the same force term as in Quinn et al. (1991), but did not adjust the initial data. To test the accuracy of the averaged model, we resolved the Earth and the Moon as two separate bodies in R5, assuming that they are point masses with only Newtonian gravitation acting between them.

The three cases — R3, R4 and R5 — were compared around 24 Myr ago in Fig. 1. Closer to the present day, the differences are small but still noticeable, as illustrated in Fig. 6. While the analytical model of Quinn et al. (1991) works quite well for a few Myr, it is not accurate enough for longer time intervals.

In principle, the analytical averaging of the lunar orbit should be supplemented by adjusting the initial positions and velocities to their averaged values. We carried out this in the case of R6, following the procedure of Quinn et al. (1991). We found very little

improvement, i.e., R4 and R6 are much closer to each other than they are to R5 (not shown).

There is one factor in the formula of Quinn et al. (1991), denoted by f in their Eq. (6), which they estimated by order-of-magnitude considerations. It is designed to take into account effects which are not included in their model, such as the eccentricities and inclinations of the orbits of the Moon and the Earth. We carried out a series of short integrations, on the time scale of tens of thousands of years, with different values of f. After a while it became apparent that f has a strong effect on the results.

We adjusted the value of f, by trial and error, until we found a better agreement with the simulation R5. Our best value for f is $f_0 = 0.8525$, used in R7 and in later cases, as opposed to the value 0.9473 calculated by Quinn et al. (1991). They note that their f is probably within 1% of the actual value. We checked their derivations and found no errors. The reason for obtaining a different f by our a posteriori method is not clear, although we suspect that Earth's orbital eccentricity is a major contributor to the discrepancy. In Table 1, averaged model (AM) refers to the case when the value $f = 0.9473$ of Quinn and colleagues is used, while modified averaged model (MAM) refers to $f = f_0$. The long-term comparison between R5 and R7 is shown in Fig. 7. The differences are still about two orders of magnitude larger than the estimated integration errors.

In order to obtain an even better model, we also derived a new formula for adjusting the initial data. The model of Quinn et al. (1991) can be regarded as the result of averaging the problem over a single, short-periodic forcing function, given by the main terms in Hill's lunar theory for the non-Keplerian motion of the Moon around the Earth in the Earth–Moon–Sun three-body problem. One can use Lie series (e.g., Varadi 1998) to compute the transformation between the initial data of the original and averaged system. We did so in R8 but found no apparent improvement (not shown). Hence, we surmise that is is best to use the modified value of $f = f_0$ in the Quinn et al. (1991) model when modeling the Earth–Moon system, at least for now.

6. COMPARISONS

While Fig. 1 shows large differences between our results and those of Laskar (1990) around 24 Myr ago, the disagreement is much smaller for the past 5 Myr (Fig. 8). The latter comparison partially validates our computations. There are no surprising features that would indicate any major problem with our physical model or integration method. Laskar's (1990) results for the past 20 Myr can be obtained from the Web site of the U.S.

National Oceanic and Atmospheric Administration's National Geophysical Data Center[4]. The U.K. Delphi Project has a data depository for marine geological paleoclimate research and provides Laskar's (1990) results for 12–34 Myr through their Web pages[5].

We compare the evolution of smoothed orbital eccentricities for the inner planets in Fig. 9. The pattern of variations changes in the case of Mars, but no visible change occurs for Earth or Venus. For Mercury, the characteristics of the time series change markedly around 65 Myr. It appears that the amplitude of an oscillatory component with a period of about 10 Myr becomes smaller as the simulations reach that particular point in time. Such transitions between different dynamical regimes are presumably induced by chaos, such as separatrix crossings or chaotic itinerancy (Arecchi et al. 1990; Otsuka 1990; Kaneko 1991; Itoh and Kimoto 1996).

Orbital inclinations relative to the system's invariable plane are plotted in Fig. 10. While the case of Mercury is the most remarkable, there are perceptible changes in the cases of Venus and Earth as well. The oscillatory patterns have more high-frequency content after 65 Myr than before. Mars, moreover, exhibits a single amplitude cycle in its oscillations, between 110 and 40 Myrs.

Laskar (1990, 1999) argued for the presence of chaos in the inner solar system through changes in secular frequencies and certain resonance variables which are not easy to interpret. Sussman and Wisdom (1992) also used resonance variables and noted the difficulty of interpreting changes in such variables. The macroscopic changes in the evolutionary patterns of Mercury's orbital elements (Figs. 9 and 10 here) are a direct proof of chaotic behavior in the inner solar system.

7. CONCLUSIONS

Despite considerable progress in the last two decades, we still do not know the details of the evolution of planetary orbits on the time scale of tens of millions of years. The present work addressed some of the most pressing issues and provides further gains in both numerical accuracy and physical insight, but there is still room for improvement.

Integration errors are now considerably smaller than the divergence of solutions due to genuine chaos in the system. The main uncertainty in the physical model is due to the

[4]http://www.ngdc.noaa.gov/paleo/forcing-orbital.html

[5]http://delphi.esc.cam.ac.uk/coredata/wwwcoredata/ODP/LEG154/orbits.html

modeling of the Earth–Moon system and its effect exceeds that of numerical errors. For the past 50 Myr, our results are quite reliable and appear to be more accurate than previous ones. We attribute this progress mainly to improvements in integration methodology and in the modeling of the Earth–Moon system.

No serious mistakes are apparent in our results, but coding errors, as well as those in handling input and output data, are not easy to avoid. The present results, therefore, need to be checked by researchers who work independently of our group and use different simulation methodologies, if possible. New integration schemes are being developed, thanks to the renewed interest of numerical analysts in planetary orbital dynamics (Sharpe 2001). Perhaps an independent study could use one of these new techniques.

Our results confirm the presence of chaos in the inner solar system. Despite being chaotic, orbital evolution in the inner solar system appears to have been quite uneventful for the past 50 Myr. The transition between different dynamical regimes around 65 Myr ago certainly deserves more attention, since it could have affected the asteroid belt and produced the bolide impact that occurred at the Cretaceous-Tertiary boundary (Alvarez et al. 1980). The macroscopic change in the evolution of Mercury's orbit makes it plausible that similar changes took place in the case of some asteroids. The rate of asteroids impacting the Earth could be related to chaotic transitions in the motion of the inner planets. This conjecture and the details of the chaotic transitions will be discussed in a separate paper.

We are indebted to Drs. D. Goldstein, K. Grazier, and W. Newman for their work on the modified Störmer scheme which we implemented. We thank J. Raeder for estimating the forces arising from solar-wind–planetary-magnetosphere interactions, whose potential relevance was first brought to our attention by G. Siscoe many years ago. We thank D. Hamilton and K. Rauch for very valuable discussions. The authors also benefited from conversations with Drs. B. Bills, R. Muller, M. Murison, M. Standish, and G. Weedon. The financial support of NSF through Grants AST96-19574 (FV) and ATM00-82131 (MG and FV) and of NASA through its Astrobiology Institute (BR and FV) is gratefully acknowledged. This is IGPP publication no. 5736.

REFERENCES

Alvarez, L. W., Alvarez, W., Asaro, F., & Michel, H. V. 1980, Science 208, 1095

Arnold, V. I. 1978, Mathematical Methods of Classical Mechanics (New York: Springer-Verlag)

Arnold, V. I. 1988, Dynamical Systems III (New York: Springer-Verlag)

Arecchi, F. T., Giancomelli, G., Ramazza, L. & Residori, S. 1990, Phys. Rev. Lett. 65, 2531

Berger A. 1978, Quaternary Research 9, 139

Berger, A., Imbrie, J., Hays, J., Kukla, G., & Saltzman, B. (eds.) 1984, Milankovitch and Climate: Understanding the Response to Astronomical Forcing. (Dordrecht, Boston: D. Reidel Pub. Co.; Sold and distributed in the U.S.A. and Canada by Kluwer; Higham, MA,)

Berggren, W. A., Kent, D. V., Swisher, C. C., & Aubry, M-P. 1995, in SEPM Spec. Publ. 54, ed. W. A. Berggren, A. William, D. V. Kent, M-P. Aubry, & J. Hardenbol (Tulsa, OK: Society for Sedimentary Geology), 129

Birchfield, G. E., & Ghil, M. 1993, J. Geophys. Res. 98D, 10385

Bretagnon, P. 1982, A&A 114, 278

Brouwer, D., & Clemence, G. M. 1961, Methods of Celestial Mechanics (San Diego: Academic Press)

Budyko, M. I. 1969, Tellus 21, 611

Duriez, L. 1982, Celest. Mech. 26, 231

Garcia-Sanchez, J., Weissman, P. R., Preston, R. A., Jones, D. L., Lestrade, J.-F., Latham, D. W., Stefanik, R. P., & Paredes, J. M. 2001, A&A 379, 634

Gear, C. W. 1971, Numerical Initial Value Problems in Ordinary Differential Equations (Englewood Cliffs, NJ: Prentice Hall)

Ghil, M. 1994, Physica D 77, 130

Ghil, M., & Le Treut, H. 1981, J. Geophys. Res. 86, 5262

Ghil, M., & Childress, S. 1987, Topics in Geophysical Fluid Dynamics: Atmospheric Dynamics, Dynamo Theory and Climate Dynamics (New York: Springer-Verlag)

Ghil, M., Varadi, F., & Kaula, W. M. 1996, in Dynamics, Ephemerides and Astronomy in the Solar System, ed. S. Ferraz-Mello, B. Morando, & J. E. Arlot (IAUS No. 172), 57

Gildor, H., Tziperman, E. 2000, Paleoceanography 15, 605

Goldstein, D. 1996, The Near-Optimality of Störmer Methods for Long Time Integrations of y"=g(y), Ph.D. Dissertation (Los Angeles: Dept. of Mathematics, Univ. of California, Los Angeles)

Goldstein, H. 1980, Classical Mechanics (2nd ed., Reading, MA: Addison-Wesley)

Grazier, K. R., Newman, W. I., Kaula, W. M., Varadi, F., & Hyman, J. M. 1995, An exhaustive search for stable orbits between the outer planets, AAS/Division of Dynamical Astronomy Meeting 1995

Grazier, K. R., Newman, W. I., Kaula, W. M., & Hyman, J. M. 1999a, Icarus 140, 341

Grazier, K., Newman, W. I., Kaula, W. M., Varadi, F., & Hyman, J. M. 1999b, Icarus, 140, 353

Hairer, E., Norsett, S. P., & Wanner, G. 1993, Solving Ordinary Differential Equations I. Nonstiff Problems (2nd revised edition; New York: Springer-Verlag)

Hays, J. D., Imbrie, J., & Shackleton, N. J. 1976, Science 194, 1121

Imbrie, J., & Imbrie, K. P. 1986, Ice Ages : Solving the Mystery (2nd edition; Cambridge, MA: Harvard University Press)

Imbrie, J. et al. 1992, Paleoceanography 7, 701

Imbrie, J. et al. 1993, Paleoceanography 8, 698

Isaacson, E., & Keller, H. B. 1966, Analysis of Numerical Methods (New York: Wiley, Dover edition, 1994).

Itoh, H. & Kimoto, M. 1996, J. Atmos. Sci. 53, 2219

Kalnay, E. 2002, Atmospheric Modeling, Data Assimilation and Predictability (Cambridge, MA:Cambridge Univ. Press)

Kaneko, K. 1990, Physica D54, 5

Kinoshita, H., Yoshida, H., & Nakai, H. 1991, Celest. Mech. Dynam. Astron. 50, 59

Laskar, J. 1990, Icarus 88, 266

Laskar, J., Quinn, T., & Tremaine, S. 1992, Icarus 95, 148

Laskar, J. & Robutel, P. 2001, Celest. Mech. Dynam. Astron. 80, 39

Laskar, J. 1999, Phil. Trans. R. Soc. Lond. A357, 1735

Lichtenberg, A. J., & Lieberman, M. A. 1992, Regular and Chaotic Dynamics (2nd ed. New York: Springer-Verlag)

Malhotra, R. 1994, Celest. Mech. Dynam. Astron. 60, 373

Milankovitch, M. 1941, K. Serb. Akad. Beogr. Spec. Publ. 132 (tranlated by the Israel Program for Scientific Translations, Jerusalem, 1969)

Murray, N., & Holman, M. 1999, Science 283, 1877

Musotto, S., Varadi, F., Schubert, G., & Moore, W. 2002, Icarus, 159, 500

Otsuka, K. 1990, Phys. Rev. Lett. 65, 329

Proakis, J. G., & Manolakis, D. G. 1996, Digital Signal Processing (Upper Saddle River, NJ: Prentice Hall)

Quinlan, G. D. 1994, Celest. Mech. Dynam. Astron. 58, 339

Quinlan, G. D. 1999, Resonances and instabilities in symmetric multistep methods, preprint, arXiv:astro-ph/9901136

Quinlan, G. D., & Tremaine, S., 1990, AJ100, 1694

Quinn, T. R., Tremaine, S., & Duncan, M. 1991, AJ101, 2287

Renne, P. R., Deino, A. L., Walter, R. C., Turrin, B. D., Swisher, C. C., Becker, T. A., Curtis, G. H., Sharp, W. D., & Jaouni, A-R. 1994, Geology 22, 783

Saha, P. & Tremaine, S. 1992, AJ104, 1633

Saha, P. & Tremaine, S. 1994, AJ108, 1962

Seidelmann, P. K. 1992, Explanatory Supplement to The Astronomical Almanac (Revised edition; Mill Valley, CA: University Science Books)

Sellers, W. D. 1969, J. Appl. Meteorology 8, 392

Shackleton, N. J., McCave, I. N., & Weedon, G. P. 1999, Phil. Trans. R. Soc. Lond. A357, 1733

Shackleton, N. J., Hall, M. A., Raffi, I., Tauxe, L., & Zachos, J. 2000, Geology 28, 447

Shu, F. H. 1992, The Physics of Astrophysics, Vol II, Gas Dynamics (Sausalito, CA: University Science Books)

Sharpe, P. W. 2001, Comparisons of High-Order Störmer and Explicit Runge-Kutta Nyström Methods for *N*-body Simulations of the Solar System, AAS/Division of Dynamical Astronomy Meeting 2001

Soffel, M. H. 1989, Relativity in Astrometry, Celestial Mechanics and Geodesy (New York: Springer-Verlag)

Standish, E. M. 1998, JPL Planetary and Lunar Ephemerides, DE405/LE405, Interoffice Memo. 312.F-98-048, Jet Propulsion Laboratory, Pasadena, California

Sussman, G. J., & Wisdom, J. 1992, Science 257, 56

Varadi, F. 1997, Numerical integrators for the gravitational N-body problem (World Wide Web)

Varadi, F. 1998, Celest. Mech. Dynam. Astron. 70, 271

Varadi, F., Ghil, M. & Kaula, W. M. 1995, in From Newton to Chaos, ed. A. E. Roy & B. A. Steves (New York: Plenum Press), 103

Varadi, F., Ghil, M., & Kaula, W. M. 1999a, Icarus 139, 286

Varadi, F., Ghil, M. & Kaula, W. M. 1999b, Celest. Mech. Dynam. Astron. 72, 187

Varadi, F. & Kaula, W. M. 1999, Planetary and Space Sci. 47, 997

Weertman, J. 1976, Nature 261, 17

Will, C. M. 1981, Theory and Experiment in Gravitational Physics (Cambridge: Cambridge Univ. Press)

Wisdom J. & Holman, M.: 1991, AJ102, 1528

Wisdom J. & Holman, M.: 1992, AJ104, 2022

Wisdom, J., Holman, M., & Touma, J. 1996. Fields Institute Communications 10, 217

Wolansky, G., Ghil, M., & Varadi, F. 1998, Icarus 132, 137

Zachos, J. C., Shackleton, N. J., Revenaugh, J. S., Palike, H., & Flower, B. P. 2001, Science 292, 274

Simulation designation	Modeling of Moon	Step size (days)	Length (Myr)
R1	barycenter	0.25	100
R2	barycenter	0.3125	212
R3	barycenter	0.25	89
R4	AM	0.3125	123
R5	resolved	0.03125	45
R6	AM+IDA	0.3125	6
R7	MAM	0.3125	207

Table 1: Summary of the simulations' properties. Except for R1, all include the effects of general relativity for each Sun–planet pair. The following abbreviations are used: AM–the averaged Earth–Moon model of Quinn et al. (1991); MAM–the modified averaged model; IDA–initial data are adjusted for consistency with the averaged model, following Quinn at al. (1991); See main text for details.

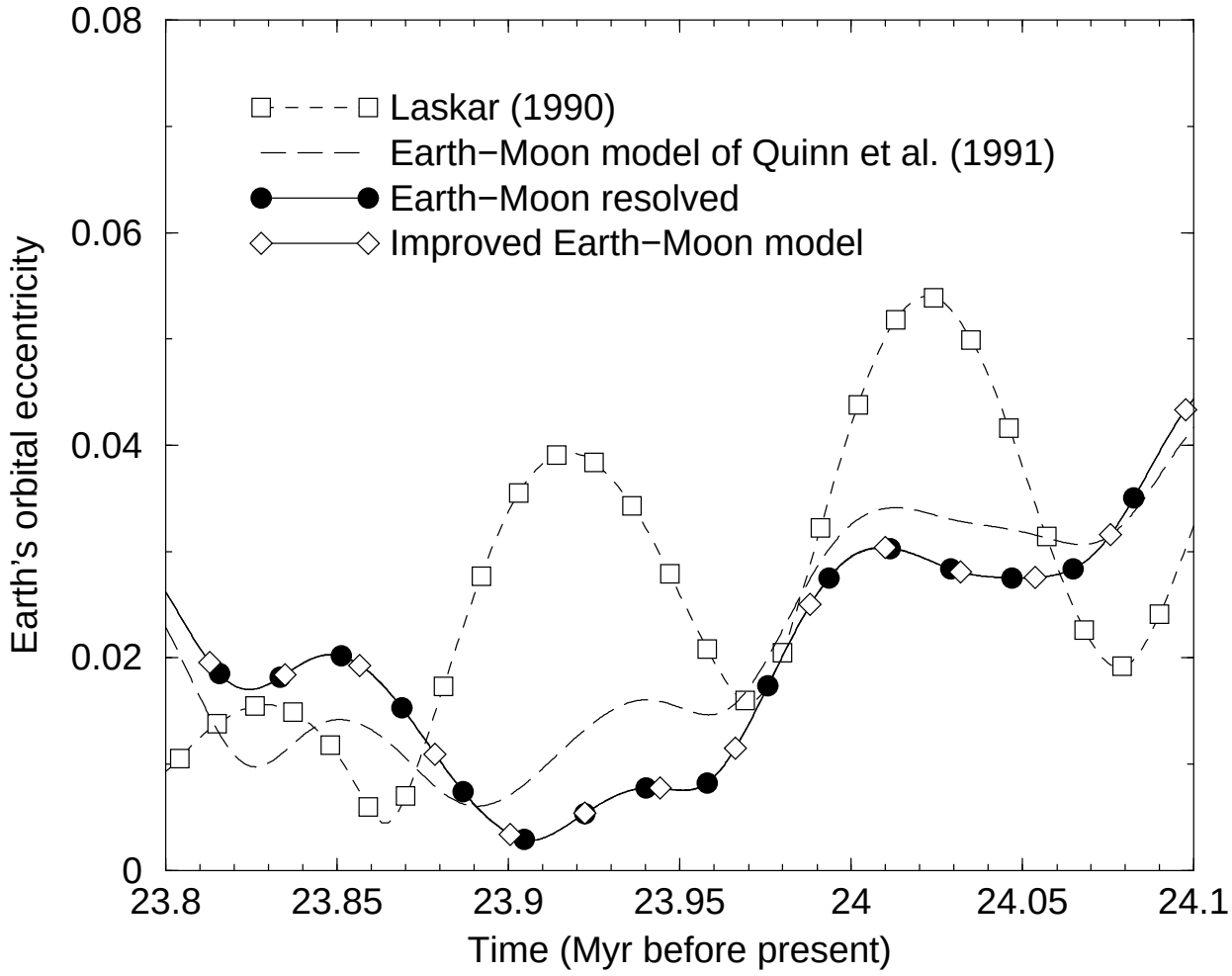

Fig. 1.— Earth's orbital eccentricity according to Laskar (1990) and our simulations with three physical models: one with the Earth–Moon model of Quinn et al. (1991), another one with these bodies resolved, and the last one with our improved Earth–Moon model. The time axis in all our figures runs from the present at the left toward the past at right, as is customary in geology and paleoclimatology.

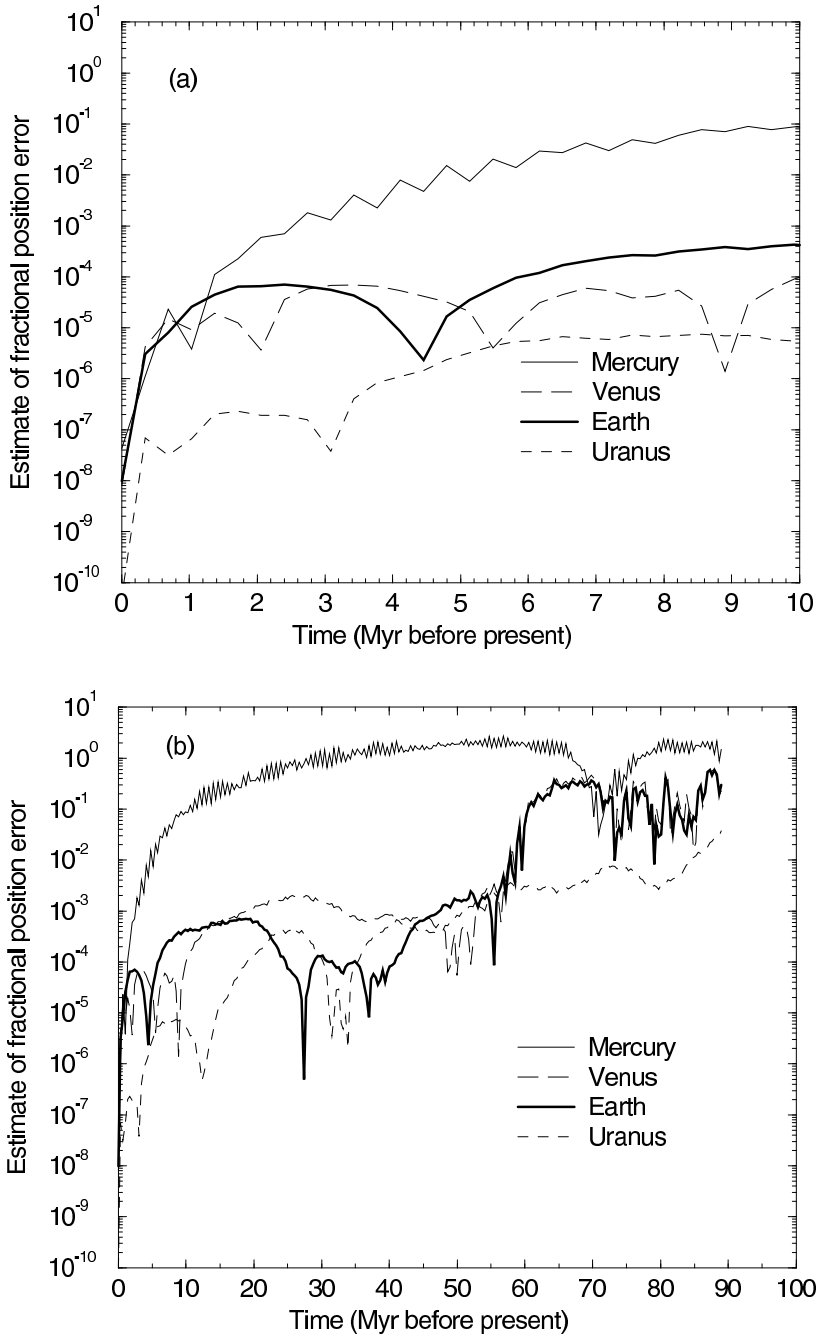

Fig. 2.— Fractional position error estimated from the difference between two integrations, R2 and R3: (a) over 10 million years (Myr); (b) over 100 Myr. The two runs differ only by their step size. Except for Mercury, the errors are less then 10^{-3} for the past 60 Myr.

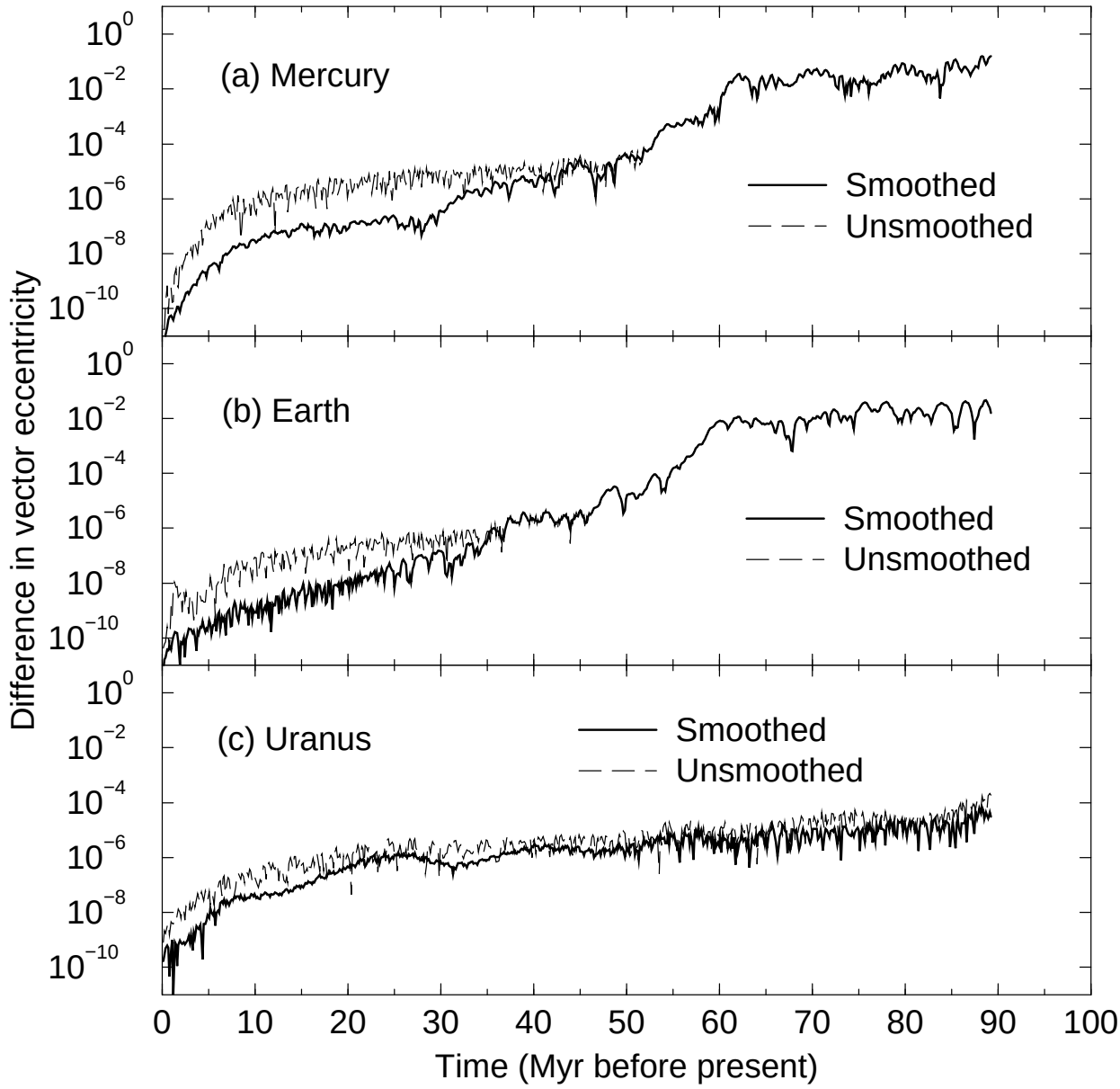

Fig. 3.— The combined effects of chaos and integration errors on the orbit of three planets: (a) Mercury, (b) Earth, and (c) Uranus. The differences between R2 and R3 in these planets' smoothed and unsmoothed vector eccentricities are plotted, i.e., the magnitude of the difference in (Laplace vectors)/(semi-major axis). See the main text for discussion.

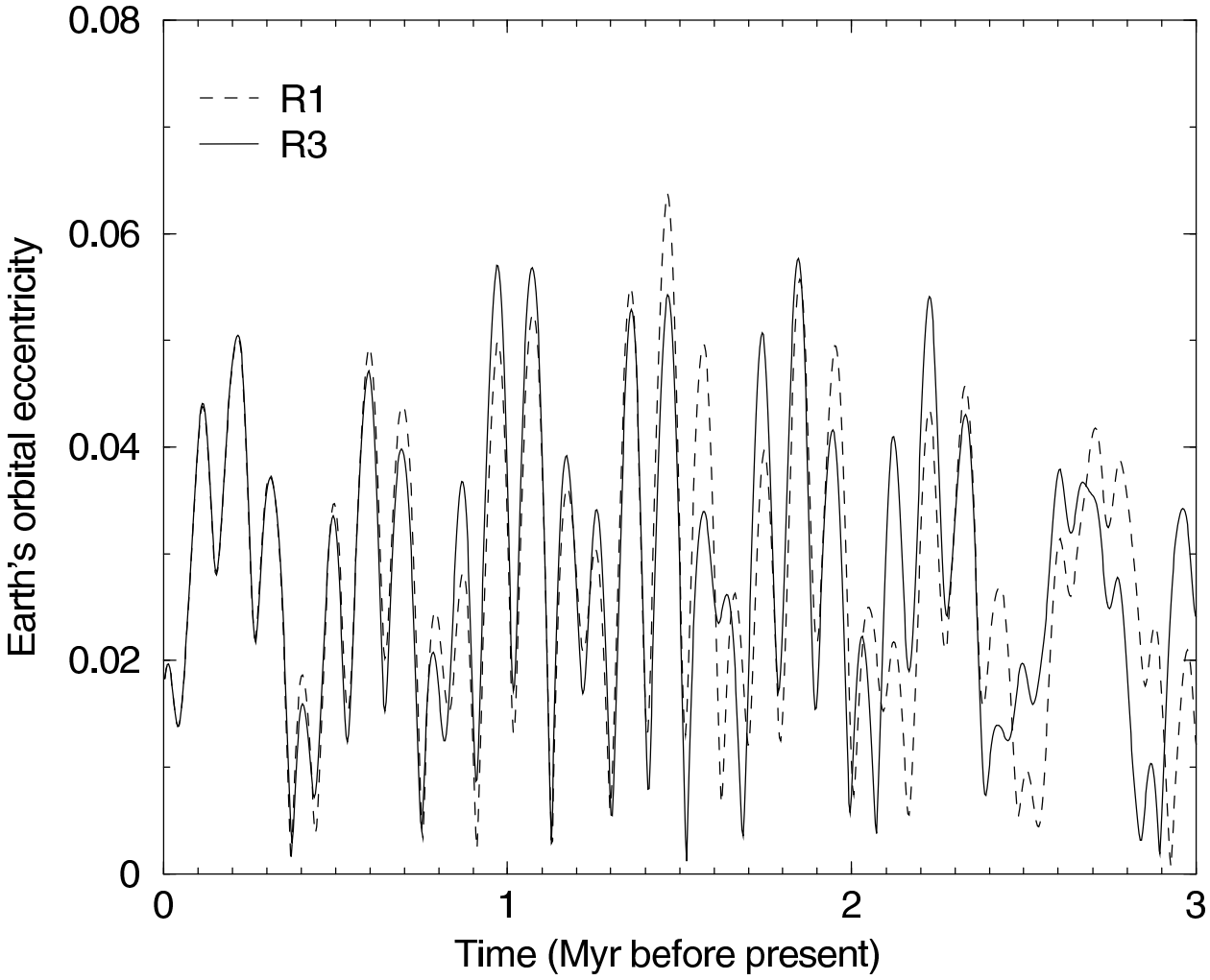

Fig. 4.— The effects of general relativity on Earth's orbital eccentricity: the two runs, R1 and R3, are identical except for R3 including these forces, while R1 does not.

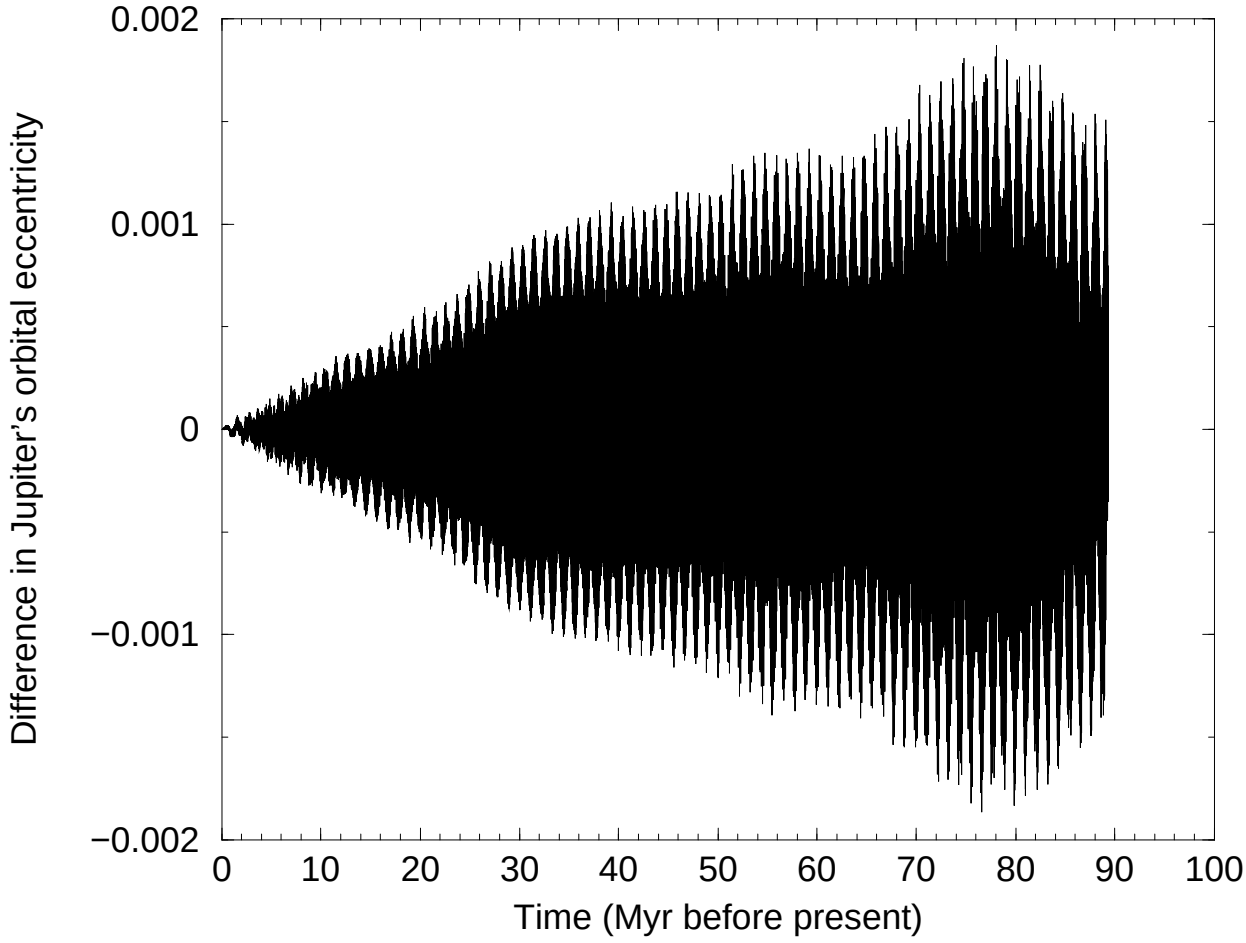

Fig. 5.— The difference in Jupiter's orbital eccentricity, between R1 and R3.

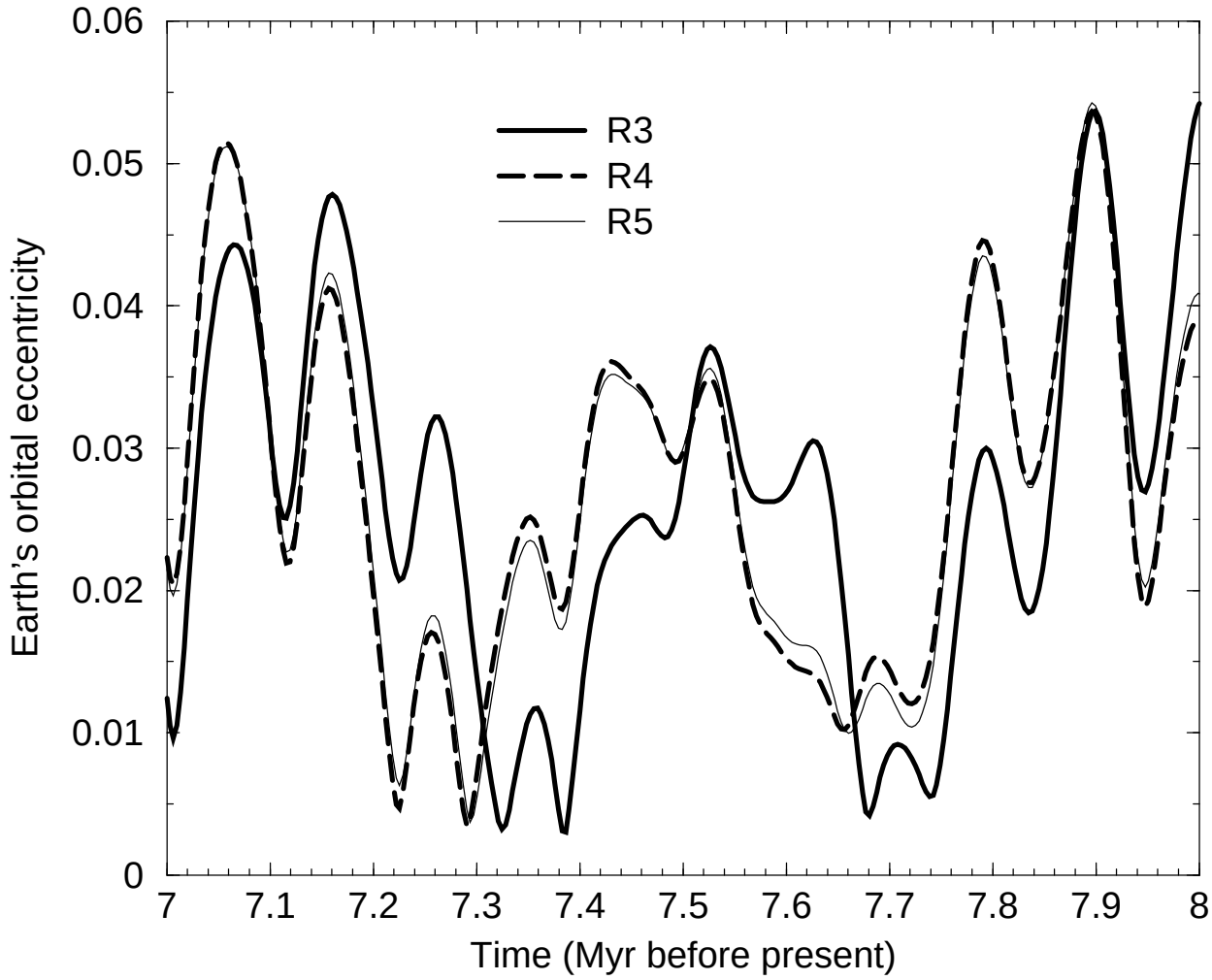

Fig. 6.— Comparison of R3, R4, R5; see Table 1 for a description of these three simulations.

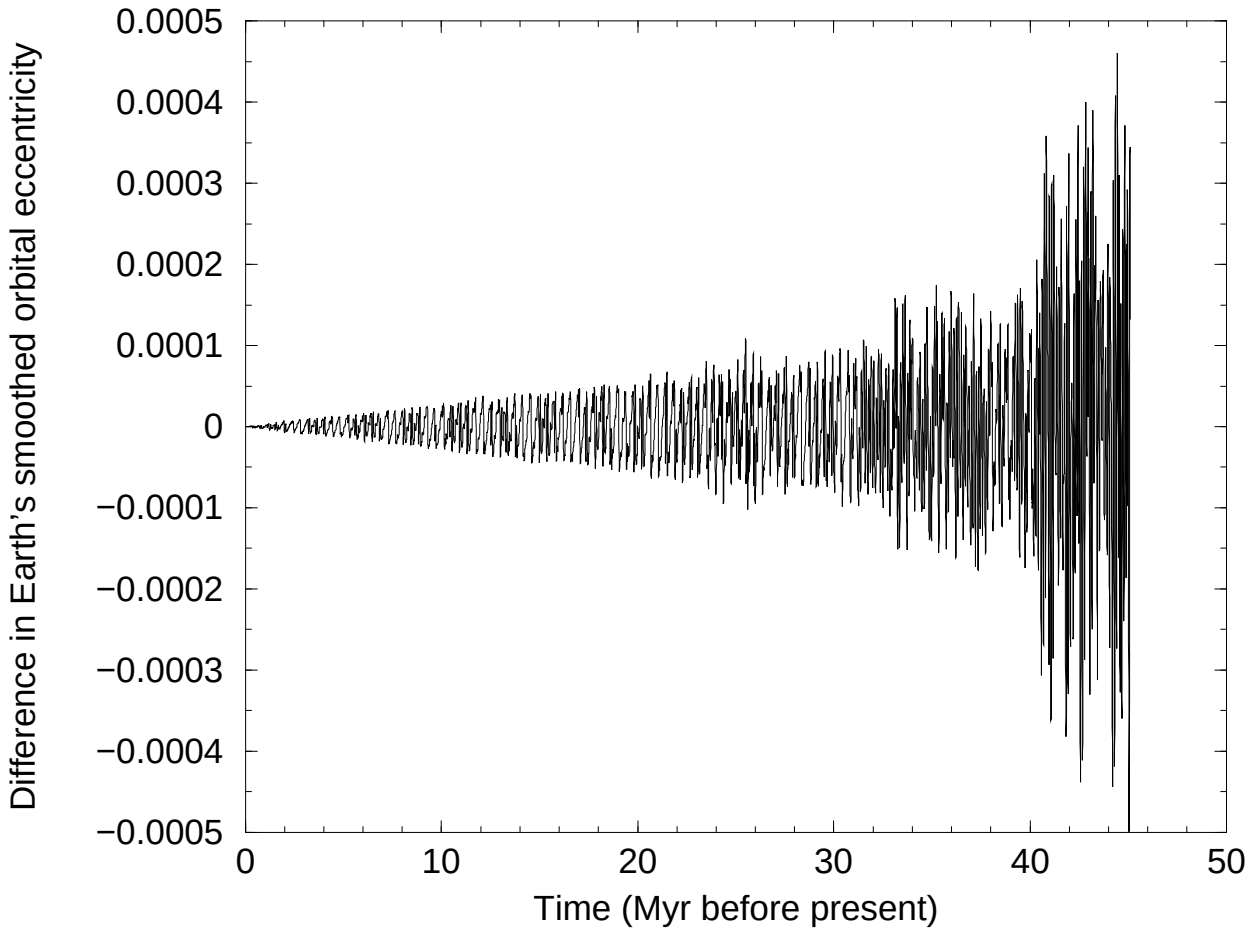

Fig. 7.— The difference in Earth's orbital eccentricity, between R5 and R7; the former model resolves the Earth–Moon system as two bodies, while the latter uses an averaged model with optimized $f = 0.8525$ (see Table 1 and main text).

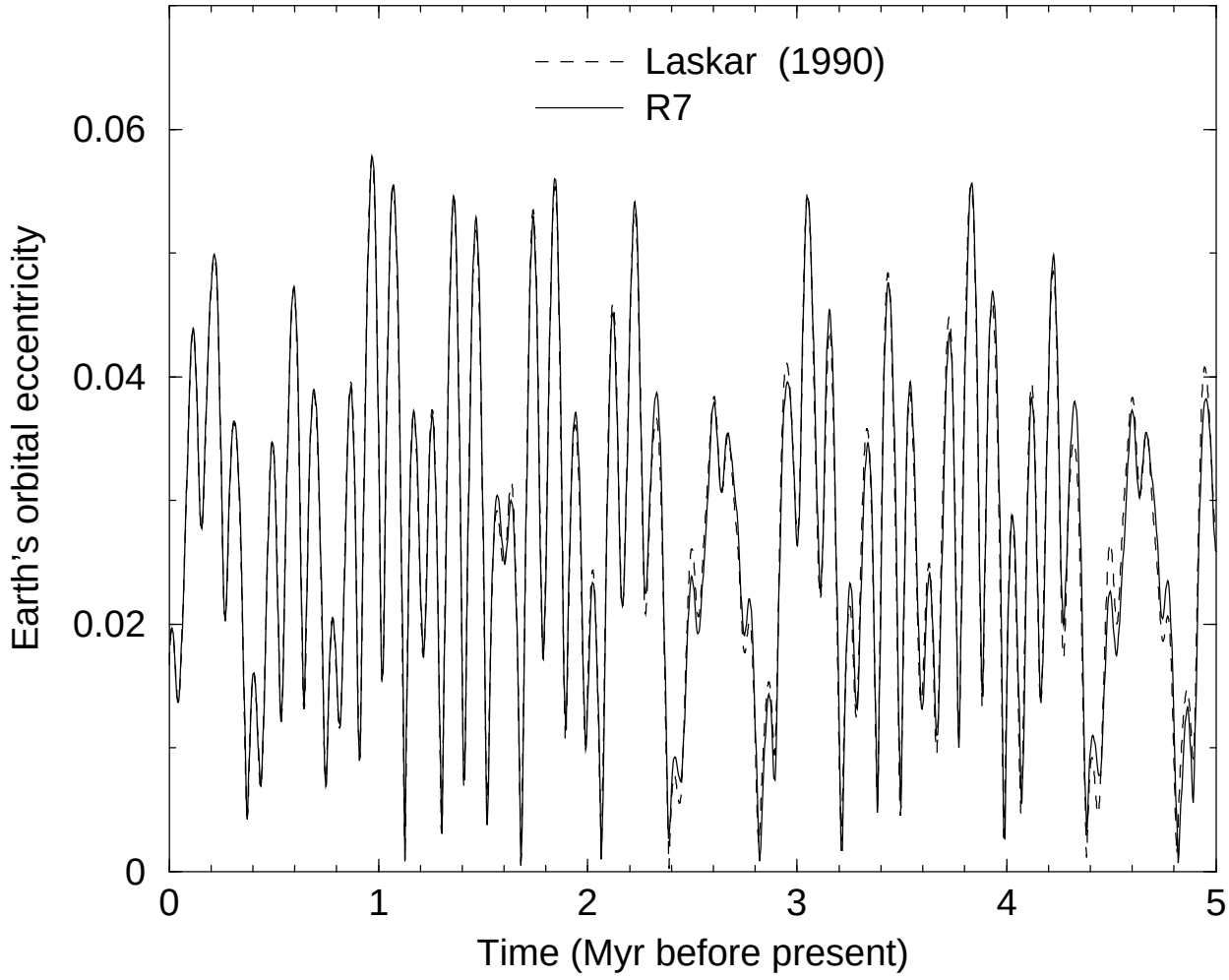

Fig. 8.— Comparison of Laskar's (1990) results and R7; the physical model of R7 most closely matches Laskar's.

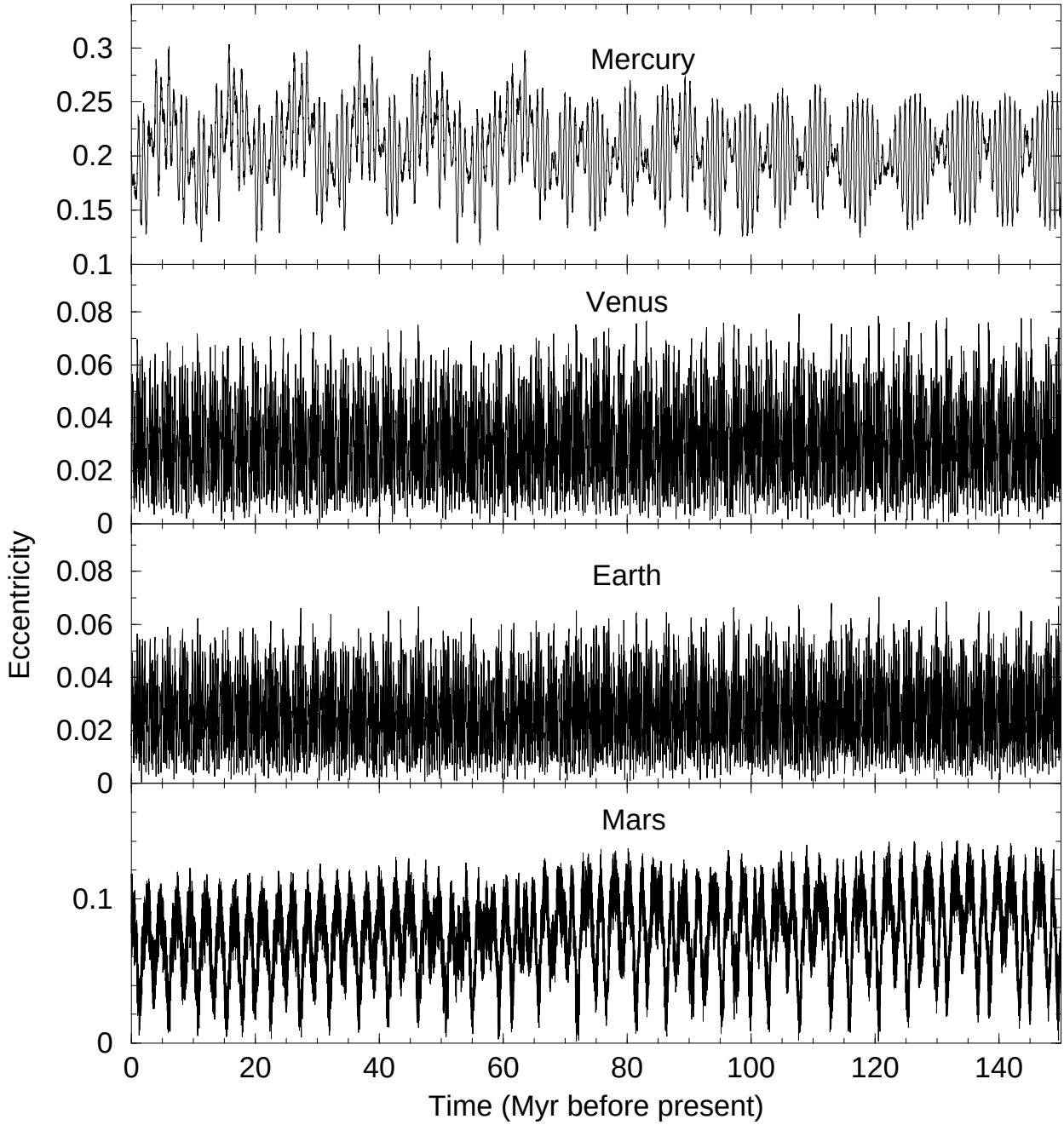

Fig. 9.— Comparison of the inner planets' smoothed orbital eccentricities in R7.

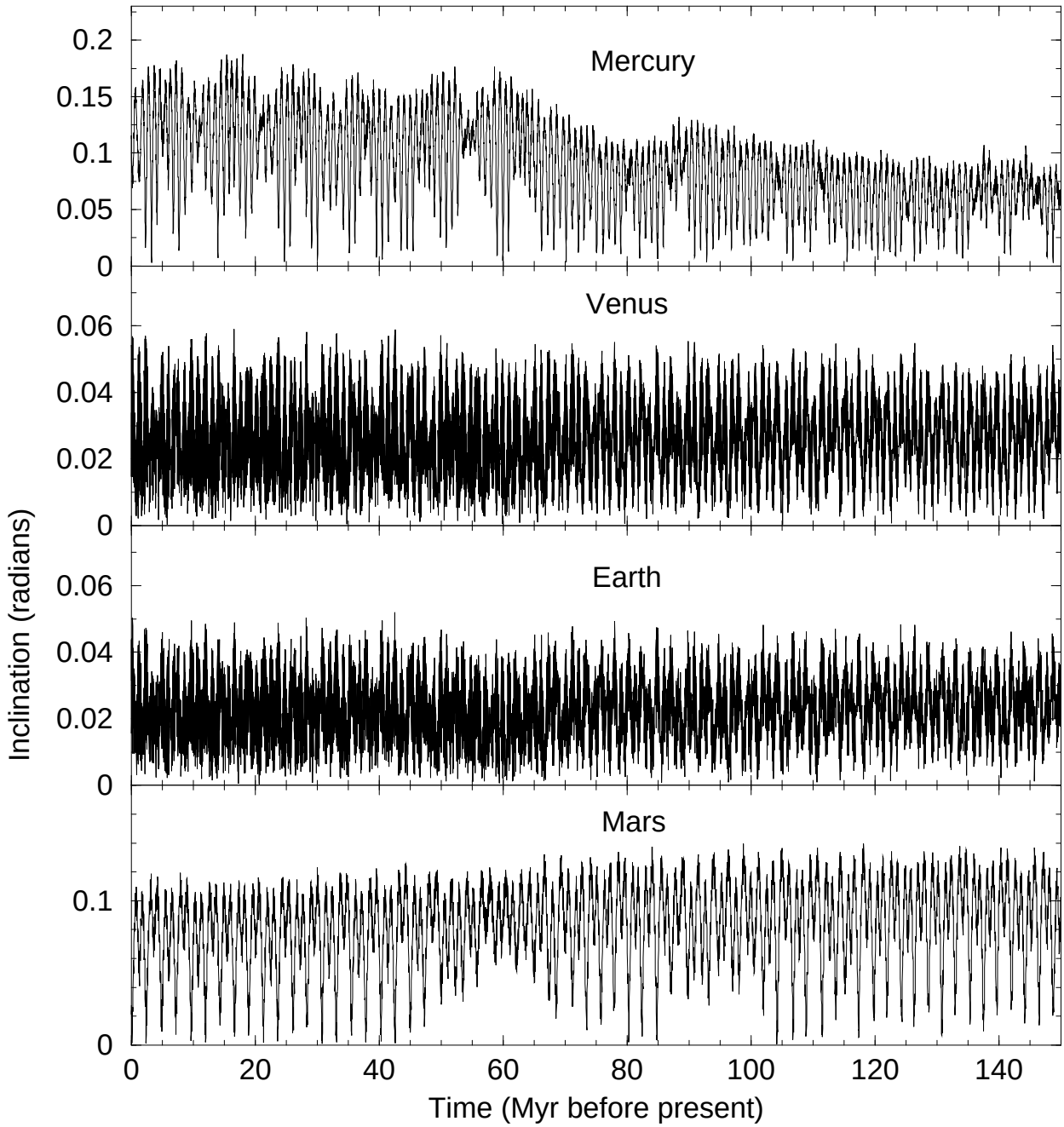

Fig. 10.— Comparison of orbital inclinations relative to the invariable plane, in R7.